Chapter 16

Engineered Tissues to Quantify Collective Cell Migration During Morphogenesis

Sriram Manivannan, Jason P. Gleghorn, and Celeste M. Nelson

Abstract

Renal development is a complex process involving the dynamic interplay of over 25 different cell types. One distinct step in this process is the formation of the ureteric tree, which develops from the repeated branching of the ureteric bud. During branching of the ureteric bud, cells migrate collectively in unison to form the complex structure of the tree. Here, we present a microlithography-based 3D culture model in which multiple identical kidney epithelial tissues are used to quantify collective cell migration during the process of branching morphogenesis.

Key words: Patterning, Engineered tissue, Persistence time

1. Introduction

The functional units of the kidney are the nephrons, which are connected together by the collecting ducts. These collecting ducts develop from the repeated branching of the ureteric bud, whereas the nephrons develop from the surrounding mesenchymal cells (1). During the initial stages of renal development, the dorsal intermediate mesoderm coalesces to form the Wolffian duct. Through cues from the surrounding mesenchyme, the Wolffian duct buds to form the ureteric bud, which then collectively migrates into the surrounding metanephric mesenchyme (MM) (1, 2). As the ureteric bud elongates, it branches to form the ureteric tree. The cells at the tips of these branches induce the surrounding mesenchyme to undergo mesenchymal-epithelial transition to form the nephrons, which elongate and segment to form the final filtration structure of the kidney (1). Movement of the ureteric bud into the MM,

Odyssé Michos (ed.), *Kidney Development: Methods and Protocols*, Methods in Molecular Biology, vol. 886,
DOI 10.1007/978-1-61779-851-1_16,

branching of the ureteric bud, and segmentation of the nephrons all rely on the coordinated migration of cell populations (3). Disrupting any of these processes affects the structure and function of the renal system, and can lead to birth defects, hypertension, or renal failure in the adult (1). Thus, it is vital to understand the role of collective cell migration during renal development.

The process of kidney development can be studied using intact animals, organ explants, or three-dimensional (3D) culture models. Whereas in vivo studies allow for examination of the phenotypic effects of genetic manipulations, live imaging of organs as they are developing is challenging in the intact animal. Organ explants help to overcome these challenges, but organs can be difficult to culture, and their growth ex vivo is often affected by dissection techniques (4). To achieve a greater degree of spatial, temporal, and physical control, simple 3D epithelial cultures have been used. These usually comprise kidney-derived cells embedded in an extracellular matrix (ECM). These models achieve the goal of producing tissues that resemble the in vivo system. However, these culture models rely on self-assembly of the cells, a process that produces tissues that are very heterogeneous in size, shape, and composition, thus making it impossible to directly compare tissues and difficult to quantify results (5).

Microlithography-based techniques can be used to overcome the problem of heterogeneity and create well-controlled, quantifiable arrays of engineered 3D tissues (5, 6). Collagen matrices with cavities of defined geometry are created using microlithographically patterned silicone molds. These cavities are filled with epithelial cells to create multiple micrometer-scale epithelial tubules initially identical in size and shape. The development of these tissues can be followed over time to investigate the control processes and collective motions that define branching morphogenesis.

2. Materials

2.1. Cell Culture

1. Madin-Darby Canine Kidney (MDCK) epithelial cells (ATCC).
2. 0.05% Trypsin-EDTA.
3. Recombinant adenovirus encoding histone 2B (H2B)-mCherry (Vector Biolabs).
4. Minimum Essential Medium (MEM) Eagle, supplemented with 10% fetal bovine serum and 1% glutamine–penicillin–streptomycin.

2.2. 3D Microlithography

1. Poly(dimethyl siloxane) (PDMS, Sylgard 184; Dow Corning).
2. Micropatterned silicon master.

3. Vacuum desiccator.
4. Ethanol.
5. 1× Phosphate-buffered saline (PBS).
6. 1% Bovine serum albumin (BSA) in PBS.
7. Collagen I, rat tail (BD Biosciences).
8. 10× Dulbecco's modified Eagle's medium Nutrient Mixture F-12 (DMEM/F12).
9. 0.1 N NaOH.
10. MEM.
11. Hepatocyte growth factor (HGF; Sigma).
12. Round glass coverslips (15 mm diameter).

2.3. Imaging and Analysis

1. Microscope incubation chamber (e.g., LiveCell; Pathology Devices).
2. Cell-tracking software (e.g., IMARIS; Bitplane).
3. MatLab or other numerical analysis software.

3. Methods

Here, we describe a 3D engineered tissue model used to quantify collective cell migration during morphogenesis of kidney epithelial cells. Collagen matrices with cavities of defined geometry are created using microlithography; epithelial cells, transduced with a fluorescent nuclear marker, are embedded in these cavities to create multiple identical micrometer-scale epithelial tubules. These tubules are imaged using time-lapse confocal microscopy and analyzed using automated cell-tracking software to study collective cell behavior during morphogenesis in a 3D environment.

3.1. Labeling Cells with a Fluorescent Nuclear Marker

1. Twelve to eighteen hours before the start of the experiment, trypsinize a plate of MDCK cells that is approximately 30% confluent (see Note 1).
2. Add recombinant adenovirus encoding H2B-mCherry at >100 MOI to the cell suspension and replate the cells (see Note 2).

3.2. Three-Dimensional Microlithography

1. Prepare the PDMS molds (stamps) and supports by mixing 60 g PDMS (10:1 w/w PDMS polymer: curing agent).
2. Mix the PDMS pre-polymer mixture thoroughly and place in a vacuum desiccator to remove air bubbles.
3. Pour 55 g of the PDMS mixture onto the silicon master and 5 g onto a polystyrene Petri dish.

4. Place the samples in an oven and bake at 60°C for 3 h.
5. Peel the PDMS from the silicon master and cut it into stamps ~10 mm × 8 mm × 2 mm in size.
6. Peel the PDMS from the Petri dish and cut it into supports ~10 mm × 8 mm × 0.4 mm in size.
7. Sterilize the PDMS stamps, supports, and coverslips with ethanol and dry them using a vacuum aspirator.
8. Coat the feature-containing surface of the stamps with ~100 μl of 1% BSA solution. After removing any air bubbles that might be present, incubate at room temperature for 30 min (see Note 3).
9. Prepare neutralized collagen by mixing 800 μl collagen, 100 μl 10× DMEM/F12, 200 μl 0.1 N NaOH, and 60 μl MEM. This volume is sufficient to make eight samples.
10. Remove the BSA from the PDMS stamps using a vacuum aspirator and rinse the stamps twice with ~25 μl of neutralized collagen.
11. Add ~40 μl of neutralized collagen to the stamp. Flip the stamp over onto supports that are placed ~8 mm apart.
12. Incubate at 37°C for 30 min to allow the collagen to gel.
13. Trypsinize the H2B-mCherry-transduced cells to prepare a concentrated suspension and keep on ice.
14. Place ~30 μl of neutralized collagen on top of the 15-mm coverslips and incubate at 37°C for 10 min.
15. Use sterilized tweezers to remove the PDMS stamps gently from the molded collagen gels without distorting the cavities.
16. Add one drop of the cell suspension (~25 μl) to the collagen gel and wait for the cells to settle into the cavities (see Note 4).
17. Once the cavities are full, wash off excess cells by pipetting 400 μl of cold media across the surface of the collagen gel.
18. Repeat the washing step as needed to remove the excess cells.
19. Place the sample at 37°C for 10 min to allow the cells to attach to the collagen.
20. Place the collagen-coated glass coverslip on top of the sample.
21. Add 2 ml of culture media to the sample.
22. Place the sample in a 37°C incubator overnight to allow the formation of MDCK tubules (see Note 5).

Figure 1 summarizes the procedure of creating epithelial tubules and Fig. 2 shows MDCK tubules created using this method.

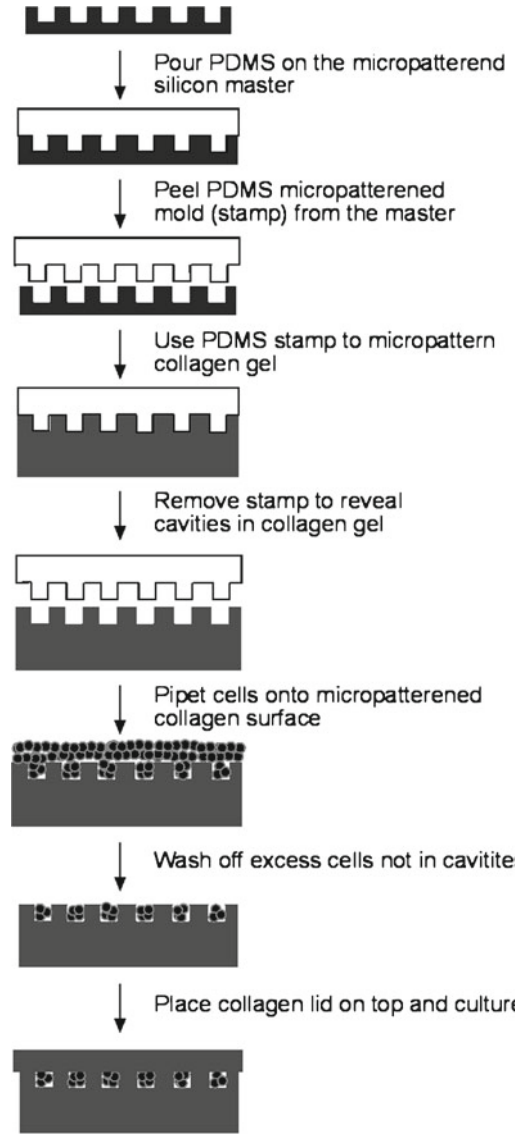

Fig. 1. Schematic of 3D microlithography procedure.

3.3. Imaging and Tracking

1. Equilibrate the microscope incubation chamber to 37°C, 5% CO_2, and ~90% relative humidity.
2. Place the sample inside the incubation chamber and choose the locations to be imaged using the microscope software (see Note 6).
3. Bring each tubule to be imaged in focus and set the Z steps (see Note 7).
4. Image for 12–24 h at 5–10-min intervals (see Note 8).
5. To analyze the images, import the time-lapse image sequence into IMARIS (see Note 9).

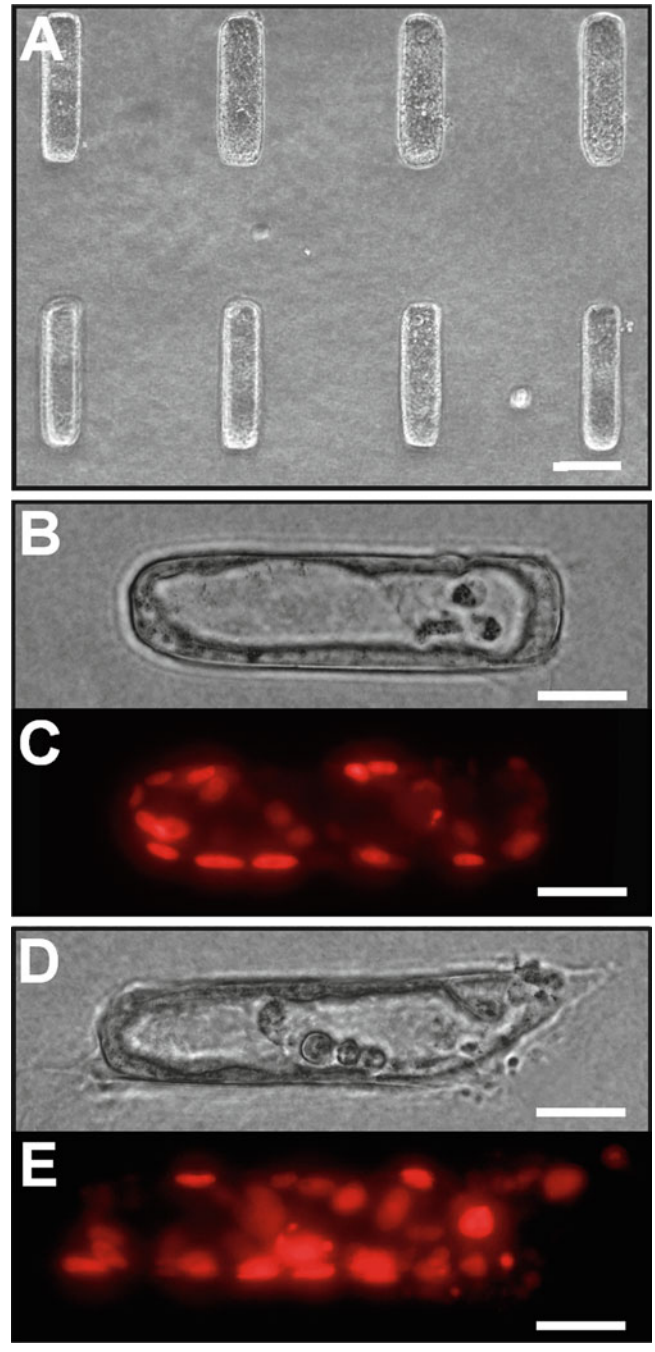

Fig. 2. After overnight incubation, the cells embedded in the collagen gel organize to form a tubule. (**a**, **b**) Phase images and (**c**) fluorescence image of quiescent MDCK tubules expressing H2B-mCherry. (**d**) Phase image and (**e**) fluorescence image of H2B-mCherry-expressing MDCK tubules induced to undergo branching by addition of 10 ng/ml HGF. Scale bars, 100 μm (**a**), 50 μm (**b**–**e**).

6. Use "Image Properties" option found under Edit menu to adjust the voxel (pixel) size and time points (see Note 10).
7. To track the cells, select "Spots" from Surpass menu and follow the Spots wizard.
8. Choose "Track Spots over time" and click next (see Note 11).
9. Under "Spots detection," enter estimated diameter of 10 μm and click next.
10. The spots algorithm will highlight the cells it has identified by placing a grey sphere (spot) on them.
11. Adjust the quality threshold to include any cells the algorithm might have missed (see Note 12).
12. After thresholding, move through the time steps of images and add spots to any cells that might have been missed in auto detection. Similarly, delete any erroneously placed spots.
13. Upon finishing the spots wizard, the software will display the trajectories of the cells (see Note 13).

    Figure 3 shows a tubule that was tracked using IMARIS.

3.4. Analysis

Several parameters, including mean speed, displacement, and persistence time, are commonly used to quantify cell movement. The mean speed and displacement denote the rate at which a cell is moving and the distance between its initial and final positions, respectively. The mean speed and displacement, along with other related parameters, can be exported directly from IMARIS. The persistence time is a calculation of the time it takes a cell to change its direction of travel, and thus cells with a longer persistence time change direction less often than those with a shorter persistence time. Persistence time is calculated by fitting the mean-squared displacement (the average distance a cell traveled) and other measured parameters to a persistent random walk model (7–15).

1. Export the tracking results data (including speed, *x*-displacement, *y*-displacement, *z*-displacement, and position for all cells as a function of time, and total displacement and total track length) by clicking "Export all Data" found under statistics in the spots option dialogue.
2. Calculate the mean-squared displacement ($\left\langle \mathrm{d}^2(t_i) \right\rangle$) for time interval $t_i = i \times \Delta t$ using the positional information for each cell and the following formula,

$$\left\langle \mathrm{d}^2(t_i) \right\rangle = \frac{1}{N-i+1} \sum_{n=0}^{N-i} \left[\left(x(t_{n+i}) - x(t_n) \right)^2 + \left(y(t_{n+i}) - y(t_n) \right)^2 + \left(z(t_{n+i}) - z(t_n) \right)^2 \right],$$

   where N = number of observations and $5 \le i \le (N/2)$ (see Note 14).

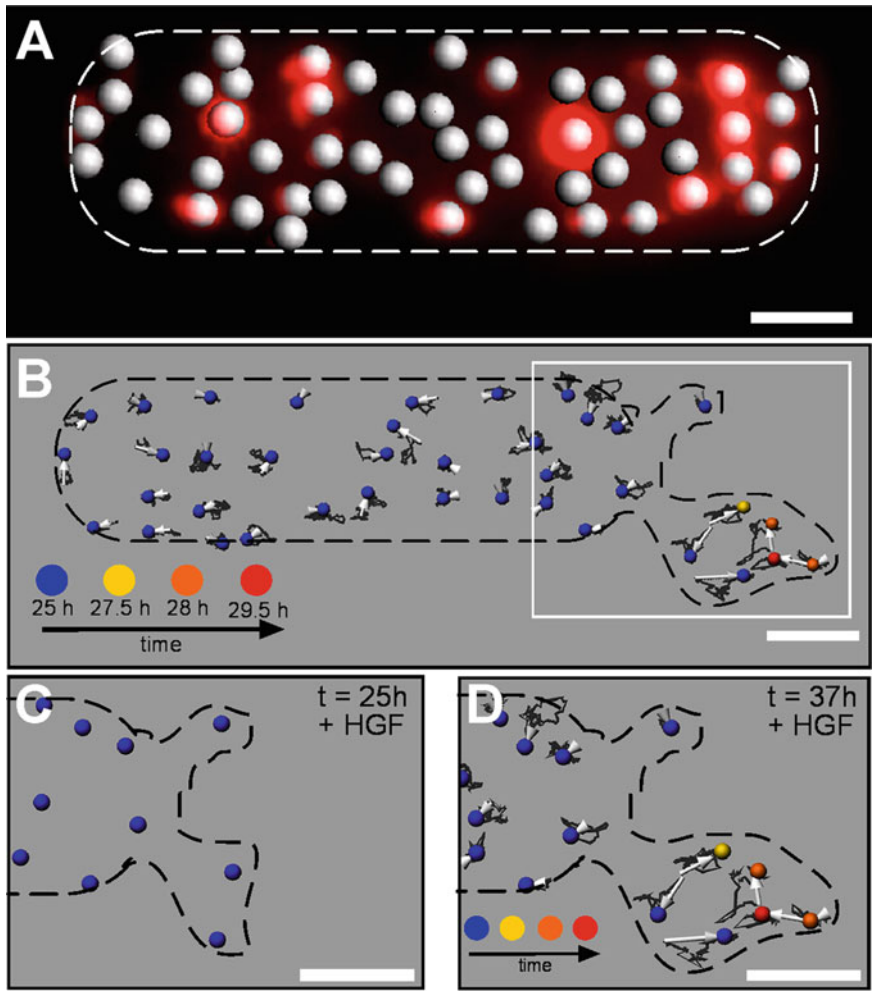

Fig. 3. (**a**) MDCK tubule in the process of branching with the nuclei identified (*white spots*). *Dotted line* denotes boundary of the tubule. (**b**) Nuclei displacement vectors (*white arrows*) and tracks (*black lines*) for cells of an MDCK tubule over 12 h. Fewer nuclei are identified for clarity and *spot colors* denote the age of cells. The branch (*boxed region*) is shown in panels (**c**, **d**). Branch of the tubule at the (**c**) start and (**d**) end of imaging. Scale bars, 30 μm.

3. Calculate persistence by fitting the data to the persistent random walk model using a least squares regression method.

$$\left\langle \mathrm{d}^2(t) \right\rangle = 2V^2P\left[t - P\left(1 - \exp\left(-\frac{t}{P}\right)\right)\right],$$

where V = average cell speed and P = persistence time.

For MDCK tubules imaged for 12 h at 10-min intervals starting 24 h after treatment with 10 ng/ml of HGF, we found that the cells moved with a velocity of ~14 μm/h and a persistence time of ~18 min. Over this time period, the branches are just starting to

form. To observe robust branching, we recommend imaging and tracking for longer time periods (~24 h) with short intervals.

4. Notes

1. It is difficult to transduce MDCK cells without first suspending them. Transduction becomes even more difficult as their confluence increases and they form a monolayer (16).
2. We found that adding ~700 MOI gives 100% transduction after 15 h for this particular virus; if the transduction is not 100%, increase the amount of virus added.
3. To remove air bubbles, try gently scratching them off using a pipette tip. Incubating the BSA-coated stamps at 4°C overnight will also help to remove bubbles.
4. It takes about 60–90 s for the cells to fill the cavities. Gently shaking the dish will help the cells fall into the cavities.
5. After ~12 h, the MDCK tubules should be fully formed.
6. Pretreating samples with 5–10 ng/ml of HGF increases the motility of the cells (17).
7. Set Z step ~2 μm and image 60 μm above and below zero location.
8. The interval of time between subsequent images should be chosen such that it is much smaller than the persistence time of the cells being imaged.
9. When importing the sequence of images into IMARIS, specify that the images are time steps by clicking on "Setting" in the open file window and selecting T.
10. Voxel size depends on the microscope, camera, and the objective used.
11. Reducing the area of interest using "Segment only a Region of Interest" can increase automated spot detection speed and decrease computational resources.
12. Lowering the quality threshold allows the software to identify faint signals as cells to track, but this also increases noise.
13. To correct for drift during imaging, click "Drift Correction" found under Edit in the spots menu.
14. Mean-squared displacement is not calculated for time intervals shorter than $5 \times \Delta t$ or longer than $(N/2) \times \Delta t$ to minimize errors. These errors may be caused by incorrect choice of Δt at short intervals or by the overlapping interval calculations of MSD at long intervals (11, 18).

Acknowledgments

We thank Nikolce Gjorevski for assistance with the imaging and tracking software. This work was supported in part by grants from the NIH (CA128660 and GM083997), Susan G. Koman for the Cure (FAS0703855), the David and Lucile Packard Foundation, and the Alfred P. Sloan Foundation. C.M.N. holds a Career Award at Scientific Interface from the Burroughs Wellcome Fund.

References

1. Costantini F, Kopan R (2010) Patterning a complex organ: branching morphogenesis and nephron segmentation in kidney development. Dev Cell 18:698–712
2. Pohl M, Stuart RO, Sakurai H, Nigam SK (2000) Branching morphogenesis during kidney development. Annu Rev Physiol 62:595–620
3. Vasilyev A, Liu Y, Mudumana S et al (2009) Collective cell migration drives morphogenesis of the kidney nephron. PLoS Biol 7:e1000009
4. Sakurai H, Nigam SK (1998) In vitro branching tubulogenesis: Implications for developmental and cystic disorders, nephron number, renal repair, and nephron engineering. Kidney Int 54:14–26
5. Nelson CM, Inman JL, Bissell MJ (2008) Three-dimensional lithographically defined organotypic tissue arrays for quantitative analysis of morphogenesis and neoplastic progression. Nat Protoc 3:674–678
6. Nelson CM, VanDuijn MM, Inman JL, Fletcher DA, Bissell MJ (2006) Tissue geometry determines sites of mammary branching morphogenesis in organotypic cultures. Science 314:298–300
7. Zaman M, Matsudaira P, Lauffenburger D (2007) Understanding effects of matrix protease and matrix organization on directional persistence and translational speed in three-dimensional cell migration. Ann Biomed Eng 35:91–100
8. Dickinson RB, Tranquillo RT (1993) Optimal estimation of cell movement indices from the statistical analysis of cell tracking data. AIChE J 39:1995–2010
9. Dikeman DA, Rivera Rosado LA, Horn TA et al (2008) α4β1-Integrin regulates directionally persistent cell migration in response to shear flow stimulation. Am J Physiol Cell Physiol 295:C151–C159
10. Mori H, Gjorevski N, Inman JL, Bissell MJ, Nelson CM (2009) Self-organization of engineered epithelial tubules by differential cellular motility. Proc Natl Acad Sci USA 106:14890–14895
11. Rosello C, Ballet P, Planus E, Tracqui P (2004) Model driven quantification of individual and collective cell migration. Acta Biotheor 52:343–363
12. Parkhurst MR, Saltzman WM (1992) Quantification of human neutrophil motility in three-dimensional collagen gels. Effect of collagen concentration. Biophys J 61:306–315
13. Zaman MH, Trapani LM, Sieminski AL et al (2006) Migration of tumor cells in 3D matrices is governed by matrix stiffness along with cell–matrix adhesion and proteolysis. Proc Natl Acad Sci USA 103:10889–10894
14. Huang S, Brangwynne CP, Parker KK, Ingber DE (2005) Symmetry-breaking in mammalian cell cohort migration during tissue pattern formation: role of random-walk persistence. Cell Motil Cytoskeleton 61:201–213
15. ReinhartKing CA (2008) Endothelial cell adhesion and migration, In: Cheresh DA (ed) Methods in Enzymology. Academic Press, Oxford, pp 45–64
16. Arcasoy SM, Latoche J, Gondor M et al (1997) MUC1 and other sialoglycoconjugates inhibit adenovirus-mediated gene transfer to epithelial cells. Am J Respir Cell Mol Biol 17: 422–435
17. O'Brien LE, Tang K, Kats ES et al (2004) ERK and MMPs sequentially regulate distinct stages of epithelial tubule development. Dev Cell 7:21–32
18. Shreiber DI, Tranquillo RT (2006) Three-dimensional, quantitative in vitro assays of wound healing behavior. In: Celis JE (ed) Cell biology: a laboratory handbook, 3rd edn. Academic Press, Oxford, p 2328